AD-A243 473

(1)

ESL-TR-90-44

FEASIBILITY OF A 6-INCH SPLIT HOPKINSON PRESSURE BAR (SHPB)

E. L. JEROME

SVERDRUP TECHNOLOGY, INC.
P. O. BOX 1935
EGLIN AFB FL 32542

JANUARY 1991

FINAL REPORT

MAY 1989 - JULY 1990

APPROVED FOR PUBLIC RELEASE : DISTRIBUTION UNLIMITED

91-17540

AFESC

AIR FORCE ENGINEERING & SERVICES CENTER
ENGINEERING & SERVICES LABORATORY
TYNDALL AIR FORCE BASE, FLORIDA 32403

91 1210 060

NOTICE

PLEASE DO NOT REQUEST COPIES OF THIS REPORT FROM HQ AFESC/RD (ENGINEERING AND SERVICES LABORATORY). ADDITIONAL COPIES MAY BE PURCHASED FROM:

NATIONAL TECHNICAL INFORMATION SERVICE
5285 PORT ROYAL ROAD
SPRINGFIELD, VIRGINIA 22161

FEDERAL GOVERNMENT AGENCIES AND THEIR CONTRACTORS REGISTERED WITH DEFENSE TECHNICAL INFORMATION CENTER SHOULD DIRECT REQUESTS FOR COPIES OF THIS REPORT TO:

DEFENSE TECHNICAL INFORMATION CENTER
CAMERON STATION
ALEXANDRIA, VIRGINIA 22314

UNCLASSIFIED

SECURITY CLASSIFICATION OF THIS PAGE

REPORT DOCUMENTATION PAGE

Form Approved
OMB No. 0704-0188

1a. REPORT SECURITY CLASSIFICATION UNCLASSIFIED	1b. RESTRICTIVE MARKINGS
2a. SECURITY CLASSIFICATION AUTHORITY	3. DISTRIBUTION / AVAILABILITY OF REPORT Approved for public release Distribution unlimited
2b. DECLASSIFICATION / DOWNGRADING SCHEDULE	
4. PERFORMING ORGANIZATION REPORT NUMBER(S) TEAS-SAA-891014	5. MONITORING ORGANIZATION REPORT NUMBER(S) ESL-TR-90-44
6a. NAME OF PERFORMING ORGANIZATION Sverdrup Technology, Inc. 6b. OFFICE SYMBOL (If applicable)	7a. NAME OF MONITORING ORGANIZATION Air Force Engineering and Services Center
6c. ADDRESS (City, State, and ZIP Code) P.O. Box 1935 Eglin AFB, FL 32542	7b. ADDRESS (City, State, and ZIP Code) HQ AFESC/RDCM Tyndall Air Force Base, Florida 32403-6001
8a. NAME OF FUNDING / SPONSORING ORGANIZATION 8b. OFFICE SYMBOL (If applicable)	9. PROCUREMENT INSTRUMENT IDENTIFICATION NUMBER F08635-86-C-0116
8c. ADDRESS (City, State, and ZIP Code)	10. SOURCE OF FUNDING NUMBERS PROGRAM ELEMENT NO. / PROJECT NO / TASK NO / WORK UNIT ACCESSION NO.

11. TITLE (Include Security Classification)

Feasibility of a 6-Inch Split Hopkinson Pressure Bar (SHPB)

12. PERSONAL AUTHOR(S)

Jerome, Elisabetta L.

13a. TYPE OF REPORT	13b. TIME COVERED	14. DATE OF REPORT (Year, Month, Day)	15. PAGE COUNT
Final	FROM May 89 TO July 90	January 1991	

16. SUPPLEMENTARY NOTATION

Availability of this report is specified on reverse of front cover.

17. COSATI CODES			18. SUBJECT TERMS (Continue on reverse if necessary and identify by block number)
FIELD	GROUP	SUB-GROUP	Split Hopkinson Pressure Bar

19. ABSTRACT (Continue on reverse if necessary and identify by block number)

The objective of this study was to assess the feasibility of a 6-Inch Split Hopkinson Pressure Bar (SHPB) using a mathematical and a numerical analysis. It was shown how by increasing the input pulse duration by the same amount as the diameter change, the wave propagation problem remains mathematically the same. This study also suggests a way to correct for friction and inertia effects.

20. DISTRIBUTION / AVAILABILITY OF ABSTRACT ☒ UNCLASSIFIED/UNLIMITED ☐ SAME AS RPT ☐ DTIC USERS	21. ABSTRACT SECURITY CLASSIFICATION UNCLASSIFIED
22a. NAME OF RESPONSIBLE INDIVIDUAL Capt. S. T. Kuennen	22b. TELEPHONE (Include Area Code) (904) 283-4932 22c. OFFICE SYMBOL HQ AFESC/RDCM

DD Form 1473, JUN 86 Previous editions are obsolete. SECURITY CLASSIFICATION OF THIS PAGE

(The reverse of this page is blank.) UNCLASSIFIED

EXECUTIVE SUMMARY

The main objective of this study was to assess the feasibility of a 6-inch Split Hopkinson Pressure Bar, SHPB, to test cementitious materials at high rates of loading. There is a need to do non-destructive tests on concrete structures, but the current SHPB's are only 2 to 3 inches in diameter and therefore they are not able to test material samples 6-inches in diameter which is the typical size of concrete specimens cored in the field.

This effort included a thorough mathematical analysis in parallel with numerical calculations. The study focused on the SHPB system, the assumptions made, their validity in a larger apparatus, and the problems and issues associated with a size change.

It was shown how by increasing the input pulse duration by the same amount as the diameter change, the wave propagation problem remains mathematically the same. However, the larger SHPB will differ from the existing smaller ones in the treatment of the specimen. Friction and inertial effects cannot be neglected any longer. This study suggests a way to correct for these effects in the data analysis phase.

The results of this study indicate that mathematically a pressure bar system can be scaled up or down to any degree, without affecting particle motion. A 6-inch SHPB is thus feasible if one can produce an input pulse of the required duration. The results also point out the potential errors in such a large system because of specimen friction and inertia.

Recommendations for further work include more numerical calculations, especially needed to fully understand the effects of the specimen. Also, it is worth considering more innovative methods of data collection and pressure input, still maintaining the basic, well proven SHPB approach.

PREFACE

This report was prepared by Ms. E. Jerome, Sverdrup, Inc., Technical Engineering Acquisition Support (TEAS) Group, P.O. Box 1935, Eglin AFB, Florida. The work was conducted for the Air Force Engineering and Services Center, Engineering and Services Laboratory, Air Base Structural Materials Branch, HQ AFESC/RDCM, Tyndall Air Force Base, Florida 32403-6001. The work was conducted under TEAS Task Order No. SAA-891014 for MSD/SAA, Eglin AFB, FL 32542-5000. Mr. J. A. Collins served as the program technical manager for MSD/SAA. Capt. S. T. Kuennen served as the program technical manager for HQ AFESC/RDCM. This report summarizes work conducted between 1 May 1989 and 31 July 1990.

This report has been reviewed by the Public Affairs Office and is releasable to the National Information Service (NTIS). At NTIS it will be available to the general public, including foreign nationals.

This report has been reviewed and is approved for publication.

STEVEN T. KUENNEN, CAPT, USAF
Project Officer

NEIL H. FRAVEL, Lt Col, USAF
Chief, Engineering Research Division

LOREN M. WOMACK, GM-14, DAF
Chief, Air Base Structural Materials Branch

FRANK P. GALLAGHER III, Colonel, USAF
Director, Engineering and Services Laboratory

A-1

(The reverse of this page is blank)

TABLE OF CONTENTS

(The reverse of this page is blank)

LIST OF FIGURES

(The reverse of this page is blank)

SECTION I

INTRODUCTION

A. OBJECTIVE

The objective of this study is to determine whether a 6-inch SHPB is feasible, whether the assumptions made in a typical 2-to-3 inch system still apply, and what major changes, problems and issues would be associated with a system that size.

The Split Hopkinson Pressure Bar, SHPB, is used to study materials at high strain-rates both in tension and in compression. An SHPB system consists of a specimen sandwiched between and in contact with two elastic bars - incident and output bar. The incident bar is impacted by a striker bar at a known velocity causing a pressure pulse to travel down the bar. This wave is partially reflected at the incident bar/specimen interface, partially reflected at the specimen/output bar interface, and the remainder is transmitted to the output bar. Two strain gages usually record the response of the reflected, transmitted, and incident pulse. From these data stresses, strains and strain-rates in the specimen can be computed as a function of time.

Although different sizes of SHPB have been built, the largest existing one is 3 inches in diameter. There are reasons behind this size limitation: it is generally assumed the wave propagation is one-dimensional, implying a high length to diameter ratio. This apparatus has been around since the late 1940s when techniques and instrumentations were not as sophisticated as they are today. Furthermore, there really never was a need to test a material specimen larger than 3 inches in diameter. The Air Force has been interested in concrete structures for years and the only concrete specimens it can test today at the strain rates typical of weapon's blast pressures are in the 2-to-3 inch diameter range. Unfortunately, these

specimens cast in a laboratory are significantly different from the type of concrete found on runways, shelters and other structures. The major difference is the aggregate size. Therefore, to obtain reliable results, full-scale destructive tests usually need to be performed. This is both time consuming and costly. There is then a need to use an SHPB type apparatus to test concrete specimens, usually about 6 inches in diameter, cored or cast directly in the field.

B. BACKGROUND

The mechanical behavior of concrete and other cementitious materials at high rates of loading has been the subject of many investigations in recent years. Understanding how the mechanical properties of these materials depend on the rate at which stresses are applied is essential to improve the design of protective structures subjected to non-nuclear weapons effects.

The SHPB has proven to be a very effective and useful tool to conduct material response studies since Kolsky [1] described its use in 1949. Detailed discussions of how a typical system works can be found in numerous papers including Hauser, Simmons and Dorn [2], Lindholm [3], Malvern and Ross [4], Robertson, Chou, and Rainey [5] and many others.

Because of the inherent difficulties associated with a system of this kind, an idealized one-dimensional wave theory is commonly assumed, where stress is uniformly applied over each cross section, plane cross sections remain plane during motion and stress and strain are uniform throughout the length of the specimen. The above assumptions are adequate if the length of the bar greatly exceeds the diameter to insure no end effects, but factors like radial and axial inertia effects and friction between the specimen and the bars can cause erroneous results if care is not used in either conducting the experiment or analyzing the data.

Approximate corrections for the calculated one-dimensional stress have been formulated to account for inertial and frictional effects. Kolsky [6] introduced a correction for radial inertia. Davies and Hunter [7] discussed both friction and inertia effects. Other papers of interest on this subject are those by Rand [8], Dharan and Hauser [9], Samanta [10], Jahsman [11], Chiu and Neubert [12], and Young and Powell [13].

The original SHPB apparatus was devised to study materials in compression. More recently it was modified to also test specimens in both tension and torsion. Examples of these techniques are discussed by Nicholas [14], Lawson [15], Baker and Yew [16], Jones [17], Okawa [18], Rajendran and Bless [20], and Ross [21].

Follansbee and Frantz [22] used the Pochhammer-Chree frequency equation to correct the recorded pulses for dispersion as they travel down the bar assuming only the first vibrational mode is excited.

C. APPROACH

An analysis of the implications of increasing the dimensions in a SHPB, requires a thorough understanding of how the system works, what has been done and assumed in the past, and what equations govern its operation. This effort will include a review of past studies on the subject, followed by a mathematical analysis. Due to the complexity of the governing equations numerical analysis will be conducted to gain insight of the system's total response.

SECTION II

MATHEMATICAL ANALYSIS

A. SHPB ASSUMPTIONS

As discussed earlier, a one-dimensional wave theory is generally assumed in the analysis of an SHPB. The one-dimensional theory assumes longitudinal spatial variations only. Applying Newton's law for a displacement u in the x direction of the diagram below, the equation of motions for an elastic system can be written as:

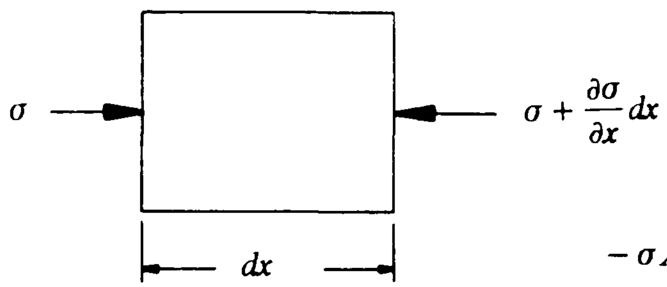

$$-\sigma A + \left(\sigma + \frac{\partial \sigma}{\partial x} dx\right) A = \rho A\, dx \left(\frac{\partial^2 u}{\partial t^2}\right)$$

or $$\frac{\partial \sigma}{\partial x} = \rho \frac{\partial^2 u}{\partial t^2} \quad \text{also} \quad \sigma = E\,\varepsilon = \frac{\partial u}{\partial x} \tag{1a}$$

where σ is the stress, E is Young's modulus, ε is strain, t is time and ρ is the density of the material. Equation (1a) can be rewritten as follows:

$$\frac{\partial^2 u}{\partial t^2} = E/\rho \frac{\partial^2 u}{\partial x^2} \tag{1b}$$

where E/ρ is the familiar elastic wave speed squared, or $E/\rho = c_o^2$. The general solution to (1b) is of the form

$$u = f(x - c_o t) + g(x + c_o t)$$

corresponding to forward and backward propagating waves. Assuming $u = g(x - c_0 t)$ only, differentiate u and obtain

$$\frac{\partial u}{\partial x} = g' \quad \text{and} \quad \frac{\partial u}{\partial t} = -c_0 g'$$

g' denotes differentiation of the function w.r.t. the argument $(x-c_0 t)$. Solving for g' from each expressing then

$$\frac{\partial u}{\partial t} = -c_0 \frac{\partial u}{\partial x} = -c_0 \varepsilon$$

strains are measured in an SHPB experiment at some distance from the specimen. To obtain the displacements, the strains are integrated directly over time, or

$$u_1 = \int_0^t -c_0 \left(\varepsilon_i - \varepsilon_r\right) dt \quad \text{and} \quad u_2 = \int_0^t -c_0 \varepsilon \, dt$$

Where the subscripts i,r, and t indicate incident, reflected and transmitted. u_1 and u_2 are the specimen's displacements at the input and output bars interfaces respectively. Let L be the length of the specimen, from the above equation the strain in the specimen is

$$\varepsilon_s = \left(u_1 - u_2\right)/L$$

and from the assumption of equal forces on each end of the specimen

$$\varepsilon_t = \varepsilon_i + \varepsilon_r$$

The specimen strain becomes $\varepsilon_s = \left(-2c_0/L\right)\int_0^t \varepsilon_r \, dt$
and the specimen strain rate is

$$\dot{\varepsilon}_s = \left(-2c_0/L\right)\varepsilon_r$$

Using Hooke's law, the stresses on either face of the specimen are

$$\sigma_{s2} = E(A/A_s)\,\varepsilon_t \quad \text{and} \quad \sigma_{s1} = E(A/A_s)(\varepsilon_i + \varepsilon_r)$$

where A/A_S is the ratio of the bar and specimen areas.

The problems with such a simplified one-dimensional theory are numerous, even for long, slender rods, and are accentuated for larger and shorter systems. First, longitudinal waves are dispersive, (wave speed is a function of frequency), even in the fundamental mode; that means what is recorded at a distance from the specimen is not the same waveform that actually arrives at the specimen. Wave dispersion can be corrected for, but it is time consuming and is not exact. The one-dimensional theory also neglects stress and displacement variations across the cross section. Since strains are measured only at the surface, this can lead to errors.

B. EQUATIONS OF MOTION

To assess the validity of this simple theory, turn to the equations of motion that govern a generalized SHPB. The equation of motion is given as

$$\nabla \cdot \tilde{T} + \rho \tilde{b} = \rho \frac{d^2u}{dt^2} \tag{2}$$

$\tilde{T}$ is the stress tensor, $\tilde{b}$ are the body forces (which are usually safely neglected), and $\frac{d^2u}{dt^2}$ is the acceleration term. In cylindrical coordinates, equation (2) becomes

$$\begin{aligned}
\rho \frac{\partial^2 u_r}{\partial t^2} &= \frac{\partial \sigma_{rr}}{\partial r} + \frac{\sigma_{rr} - \sigma_{\theta\theta}}{r} + \frac{1}{r}\frac{\partial \sigma_{r\theta}}{\partial \theta} + \frac{\partial \sigma_{rz}}{\partial z} \\
\rho \frac{\partial^2 u_\theta}{\partial t^2} &= \frac{\partial \sigma_{r\theta}}{\partial r} + \frac{1}{r}\frac{\partial \sigma_{\theta\theta}}{\partial \theta} + \frac{\partial \sigma_{\theta z}}{\partial z} + 2\frac{\sigma_{r\theta}}{r} \\
\rho \frac{\partial^2 u_z}{\partial t^2} &= \frac{\partial \sigma_{rz}}{\partial r} + \frac{1}{r}\frac{\partial \sigma_{\theta z}}{\partial \theta} + \frac{\partial \sigma_{zz}}{\partial z} + \frac{\sigma_{zr}}{r}
\end{aligned} \tag{3}$$

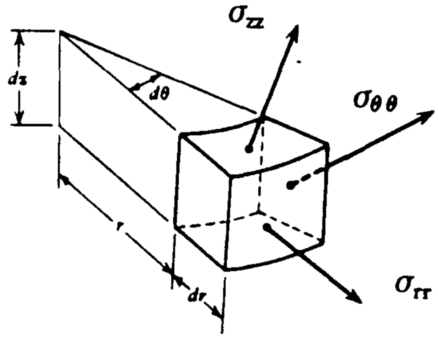

Cylindrical coordinates.

Assuming axisymmetric conditions, so that the solution is independent of theta, and using the elastic Hooke's law relationships between stresses and displacements, the two-dimensional governing equations that need to be solved in an SHPB problem, can be obtained. Specifically, using the constitutive relations,

$$\sigma_{rr} = (\lambda + 2\mu)\frac{\partial u_r}{\partial r} + \lambda\left(\frac{u_r}{r} + \frac{\partial u_z}{\partial z}\right)$$

$$\sigma_{rz} = \mu\left(\frac{\partial u_r}{\partial z} + \frac{\partial u_z}{\partial r}\right) \tag{4}$$

$$\sigma_{zz} = (\lambda + 2\mu)\frac{\partial u_z}{\partial z} + \lambda\left(\frac{u_r}{r} + \frac{\partial u_r}{\partial r}\right)$$

where λ and μ are Lame's constants, the following is obtained:

$$\rho\frac{\partial^2 u_r}{\partial t^2} = (\lambda + 2\mu)\left[\frac{\partial^2 u_r}{\partial r^2} + \frac{1}{r}\frac{\partial u_r}{\partial r} - \frac{u_r}{r^2}\right] + (\lambda + \mu)\frac{\partial^2 u_z}{\partial r\,\partial z} + \mu\frac{\partial^2 u_r}{\partial z^2}$$

$$\rho\frac{\partial^2 u_z}{\partial t^2} = \mu\left[\frac{\partial^2 u_z}{\partial r^2} + \frac{1}{r}\frac{\partial u_z}{\partial r}\right] + (\lambda + 2\mu)\frac{\partial^2 u_z}{\partial z^2} + (\lambda + \mu)\left[\frac{\partial^2 u_r}{\partial r\,\partial z} + \frac{1}{r}\frac{\partial u_r}{\partial z}\right] \tag{5}$$

The boundary conditions require no stress at the surface or

$$\sigma_{rr} = 0 \quad \text{and} \quad \sigma_{rz} = 0 \quad at\ r = a$$

where a is the radius of the bar. Also at a free end, $\sigma_{rz} = 0$ and $\sigma_{zz} = 0$ and at a rigid end, $\sigma_{rz} = 0 \;\; u_z = 0$

The initial conditions can be in the form of a step change in pressure

$$\sigma_{zz} = -P H(t)\,,\ \sigma_{rz} = 0$$

where P is a uniform pressure and H(t) is the function of time, or as a harmonic displacement of $u_z = \sin \omega t$ and $\sigma_{rz} = 0$.
Equations (5) have been solved by Pochhammer and Chree [6, 23, 27, 29] for a sinusoidal excitation. It is called the frequency equation and has the form

$$\begin{vmatrix} 2\gamma \dfrac{\partial}{\partial a} J_o(ha) & (2\gamma^2 - \dfrac{\omega^2 \rho}{\mu}) J_1(\kappa a) \\ 2\mu \dfrac{\partial^2}{\partial a^2} J_o(ha) - \dfrac{\lambda \rho \omega^2}{\lambda + 2\mu} J_o(ha) & 2\mu\gamma \dfrac{\partial}{\partial a} J_1(\kappa a) \end{vmatrix} = 0 \qquad (6)$$

where $h^2 = (2\pi/\Lambda)^2 (\rho c^2/\lambda + 2\mu - 1)$ and $\kappa^2 = (2\pi/\Lambda)^2 (\rho c^2/\mu - 1)$

Λ = ***wavelength*** , $\gamma = 2\dfrac{\pi}{\Lambda}$, and J_0 and J_1 *are the zero* and *first order Bessel functions*

C. SOLUTIONS OF FREQUENCY EQUATION

There are an infinite number of solutions to Equation (6), each corresponding to a unique mode of vibration. The solutions are exact only for an infinitely long cylinder; although, for a cylinder whose length greatly exceeds its diameter the errors are

small. Furthermore, the solutions are not explicit but rather a function relating the phase velocity c_p, the wavelength and Poisson's ratio ν. Now (6) can be written in explicity form as

$$2\mu\gamma\frac{\partial}{\partial a}J_1(\kappa a)2\gamma\frac{\partial}{\partial a}J_o(ha)-(2\gamma^2-\frac{\omega^2\rho}{\mu})J_1(\kappa a)$$
$$[2\mu\frac{\partial^2}{\partial a^2}J_o(ha)-\frac{\rho\lambda\omega^2}{\lambda+2\mu}J_o(ha)]=0 \qquad (7)$$

Making use of the following properties of the Bessels functions,

$$\frac{\partial}{\partial a}(J_o(ha))=-J_1(ha)$$

$$\frac{\partial}{\partial a}(J_1(ha))=hJ_o(ha)-J_1(ha)/a$$

Equation (7) can be rewritten as

$$4\mu\gamma^2[(\kappa J_o(\kappa a)-J_1(\kappa a)/a)(-\kappa J_1(ha))\ -(2\gamma^2-\frac{\omega^2\rho}{\mu})J_1(\kappa a)]\cdot$$
$$\cdot\left[2\mu(-hJ_0(ha)+J_1(ha)/a)-\frac{\lambda\rho\omega^2}{\lambda+2\mu}J_0(ha)\right]=0$$

which finally becomes

$$\gamma^2\kappa\frac{J_o(\kappa a)}{J_1(\kappa a)}-\frac{1}{2}\frac{1}{a}(\kappa^2+\gamma^2)+\left[\frac{1}{2}(\kappa^2-\gamma^2)\right]2\frac{J_o(ha)}{hJ_1(ha)}=0 \qquad (8)$$

Equation (8) has been numerically solved by several investigators [25,27]. The solutions for the first three frequency modes are shown in Figure 1 [22]. Mode 1, (fundamental mode), is the one of most interest for a typical SHPB. As the frequency of this mode approaches zero, or wavelength approaches infinity, the phase velocity approaches $(E/\rho)^{1/2}$ which is the elastic, one-dimensional wave speed. As the frequency becomes very large, the phase velocity approaches c_r, the velocity of Rayleigh surface waves. Although it may not be clear from Figure 1, c_p, the phase velocity, approaches c_r from the down side, implying that the phase velocity reaches a minimum which is less than the Rayleigh wave speed at some intermediate frequency.

Also, notice that the parameter h for mode 1 is always imaginary since for all frequencies $c_p < c_d$ where c_d is the dilatational wave speed in an infinite medium. Recall that

$$c_d^2 = \frac{\lambda + 2\mu}{\rho} \qquad c_t^2 = \frac{\mu}{\rho}$$

$$h^2 = (2\pi/\Lambda)^2(\rho c^2/\lambda + 2\mu - 1) \quad \text{and} \quad \kappa^2 = (2\pi/\Lambda)^2(\rho c^2/\mu - 1)$$

For very low frequencies K is real, but past roughly $\frac{a}{\Lambda}$ = 0.65, when c_p becomes less than c_t, it too is imaginary. This means that at low frequencies ($a/\Lambda < 0.65$), the displacement is mainly transverse since the set of dilatational waves exists only as a surface disturbance. At high frequencies the total displacement becomes increasingly like a pure surface disturbance.

Mode 2 and higher may be of interest in a "larger" SHPB and at high frequencies. These modes have what are called cut-off frequencies, i.e., frequencies at which the phase velocity becomes infinite. From equation (8) this implies either that γ = 0.0 or that $J_{1(Ka)}$ = 0.0. If γ = 0.0, equation (8) becomes

$$\frac{1}{2}\left(\frac{\omega_{co}}{c_t}\right)^2 \frac{1}{a} = \left(\frac{1}{2}\frac{\omega_{co}^2}{c_t^2}\right)^2 \frac{J_o(ha)}{hJ_1(ha)}$$

which can be rewritten as

$$2\frac{c_t^2}{c_d^2} = \left(\frac{\omega_{co}}{c_d}a\right)\frac{J_o(\frac{\omega_{co}}{c_d}a)}{J_1(\frac{\omega_{co}}{c_d}a)} \tag{9}$$

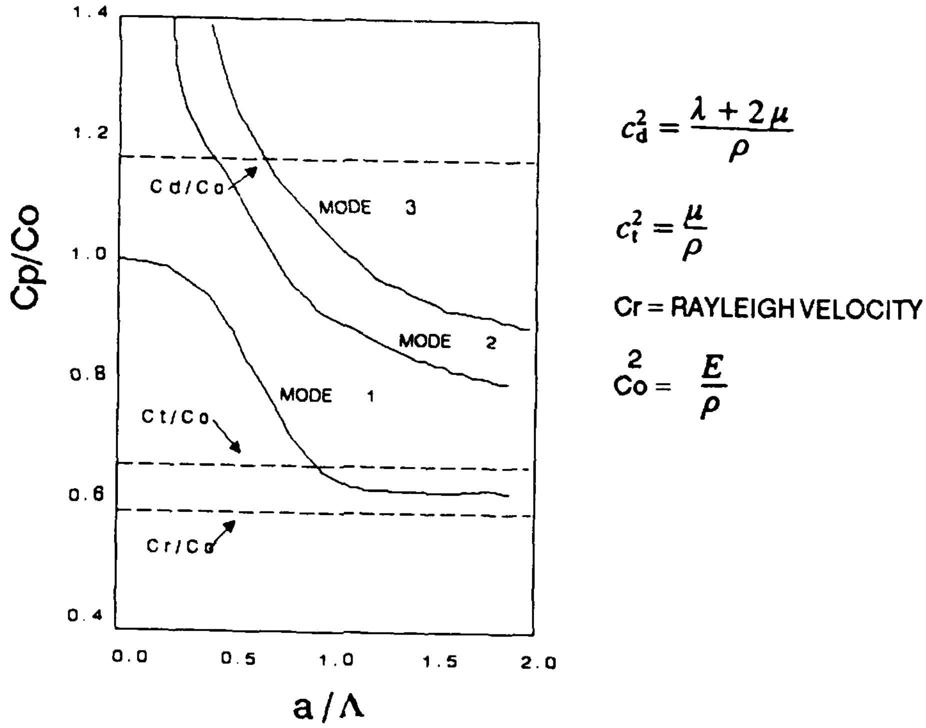

Figure 1. Pochhammer-Chree Solutions for First Three Modes.

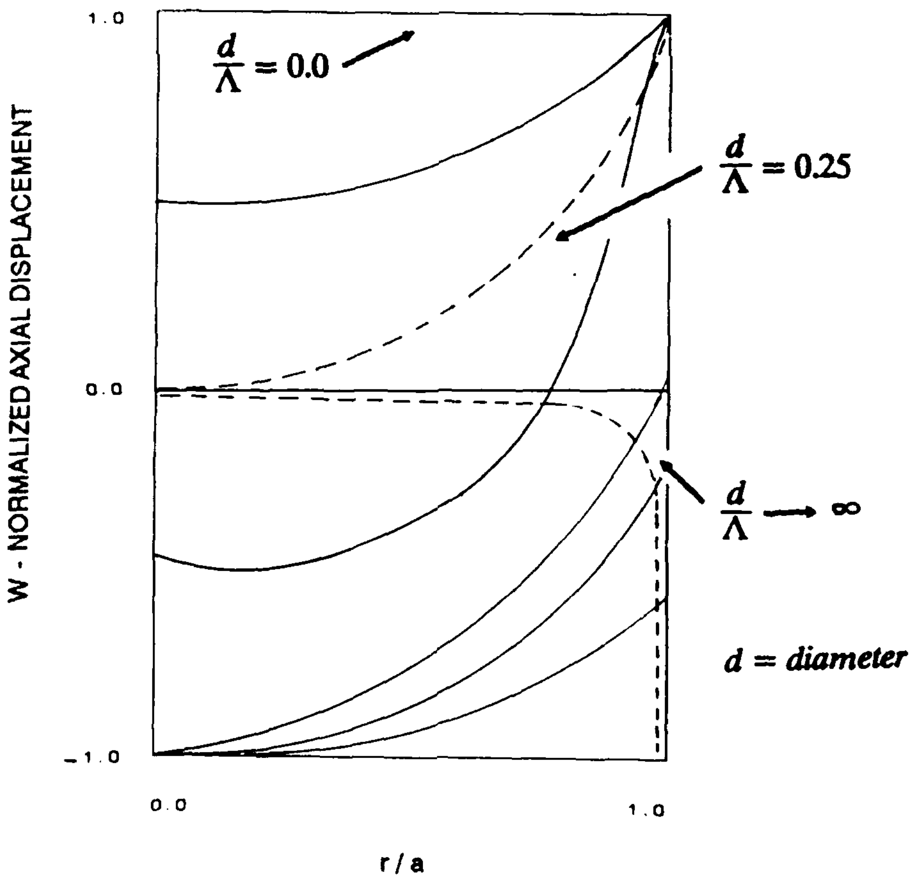

Figure 2. Longitudinal Cross-Sectional Displacement For Various values of $\frac{d}{\Lambda}$, $\mu = 0.25$.

If J_1 (Ka) = 0.0, it can be said that

$$J_1\left(\frac{\omega_{co}}{c_t}a\right) = 0.0 \tag{10}$$

Equations (9) and (10) can now be used to determine the cut-off frequencies for any mode.

From the solutions of the frequency equation, equation (8), it is possible to calculate the radial and longitudinal displacements for each mode at every frequency and Poisson's ratio within the cylinder. Bancroft [1] calculated and plotted W, the amplitude of the longitudinal displacement u_z, (i.e. $u_z = W(r)\exp(-i\gamma z)\exp(i\omega t)$ for mode 1 and $\nu = 1/4$. Results are shown in figure 2. Of interest is that W changes signs over the range a/R = 0.0 to 1.0 for values of d/Λ between approximately 0.25 and 0.4, which implies that there is a node somewhere along the radius. Also, observe that W is uniform (as expected) for d/Λ = 0.0 and that the motion is confined to the outside surface as d/Λ approaches infinity. This agrees with the observations made earlier about mode 1 response in general.

Numerous other approximate methods of varying degrees of complexity have been developed to mathematically treat a SHPB system. They fall somewhere in between the simple one-dimensional theory and the two-dimensional, coupled differential equations just presented. Unfortunately, those that show good agreement with the exact solution have very complicated descriptive equations, while those simple equations agree with the exact theory only over a very limited frequency range.

When computers were not readily available and usable, a large number of approximate theories were developed. Most important to this study are the different methods and approaches used to

derive these theories. As already discussed, the simplest analysis is to assume uniform and purely axial stress. This leads to the familiar one-dimensional wave equation

$$\frac{\partial^2 u_z}{\partial t^2} = E/\rho \, \frac{\partial^2 u_z}{\partial z^2} \tag{11}$$

which predicts that waves of all frequencies travel at the same constant velocity $c_o = (E/\rho)^{1/2}$. Of course, this is only true for very low frequencies (long wavelength). A better approximation to this theory introduces a correction for the radial motion by considering the inertia of the cross section. The approach involves the use of Hamilton's principle which states that the variations of the integral of the total energy with respect to time is zero. Specifically

$$\delta \int (T - V)\, dt = 0 \tag{12}$$

The total energy, (T - V), is the sum of the kinetic and the potential energy and for the cylinder it can be written as:

$$\int_0^L [\, \tfrac{1}{2} \rho A \left(\left(\frac{\partial u_z}{\partial t} \right)^2 + (\nu R)^2 \left(\frac{\partial^2 u_r}{\partial z \, \partial t} \right)^2 \right) + \tfrac{1}{2} E A \left(\frac{\partial u_z}{\partial z} \right)^2]\, dz \tag{13}$$

kinetic energy　　　　　potential (strain) energy

where L is the length of the cylinder, R is the radius of gyration about the z-axis,   is Poisson's ratio, and the velocities in the z and r directions are respectively

$$\frac{\partial u_z}{\partial t} \quad \text{and} \quad \frac{\partial u_r}{\partial t}$$

But u_r can be assumed to be of the form $(-\nu r \frac{\partial u_z}{\partial z})$ so that

$$\frac{\partial u_r}{\partial t} = -\nu r \frac{\partial^2 u_z}{\partial z\, \partial t}$$

The result of substituting Equation (13) into (12) and solving the integration by parts is as follows:

$$\rho \left[\frac{\partial^2 u_z}{\partial t^2} - (\nu R)^2 \frac{\partial^4 u_z}{\partial^2 z\, \partial^2 t} \right] = E \frac{\partial^2 u_z}{\partial z^2} \qquad (14)$$

This equation gives a better approximation to the exact theory than Equation (11) at low frequencies. However, for short waves the errors become considerable.

A third approximate theory developed by Love [29] is based on the exact characteristic Equation (8), where the Bessels functions are expanded in power series. If a, the radius of the cylinder, is small enough to that ha and Ka are small compared to unity, then powers of ha and Ka higher than the second can be neglected.

That is

$$J_O(Ka) = 1 - 1/4\ (Ka)^2$$

$$J_1(Ka) = 1/2\ (Ka)$$

and the following is then obtained:

$$c_n = \sqrt{\frac{E}{\rho}}\left(1 - \frac{1}{4}\nu^2\gamma^2 a^2\right) \tag{15}$$

$$\frac{c_n}{c_o} = 1 - \nu^2\pi^2\left(\frac{a}{\Lambda}\right)^2 \qquad where \;\; c_o = \sqrt{\frac{E}{\rho}} \tag{16}$$

This theory agrees fairly well with the exact theory up to values of $\frac{a}{\Lambda}$ = 1 but then rapidly diverges. The assumptions that Ka and ha are small compared to unity imply that the wavelengths of the vibrations are large compared to the radius of the cylinder.

Another common theory was developed by Mindlin and Herrmann [26]. It considers shear stresses and strains by assuming first that the radial displacement is of the form

$$u_r = (r/a)\ u(z,t)$$

with u_θ = 0 and u_z = w(z,t). Forces and moments are then calculated from standard engineering mechanics formulas and corrected for shear and inertia by introducing factors K_1 and K_2. This leads to equations of the form

$$a^2 K_1^2 \mu \frac{\partial^2 u}{\partial z^2} - 8 K_2^2 (\lambda + \mu)\, u - 4\, a K_2^2 \lambda \frac{\partial \omega}{\partial z} = \rho\, a^2 \frac{\partial^2 u}{\partial t^2} \tag{17}$$

$$2\, a \lambda \frac{\partial u}{\partial z} + a^2 (\lambda + 2\mu) \frac{\partial^2 \omega}{\partial z^2} = \rho\, a^2 \frac{\partial^2 \omega}{\partial t^2}$$

Substituting

$$u = A \exp(-i\gamma z)\, \exp\left(i\,\omega\, t\right)$$

and

$$w = B \exp(-i\gamma z)\, \exp\left(i\,\omega\, t\right)$$

into Equation (17), two equations in A and B are obtained which can be eliminated to again obtain a characteristic equation which relates phase velocity and frequency for the first two modes. By

adjusting K_2 and K_1, a very good approximation can be obtained for mode 1. Mode 2 on the other hand shows considerable deviation from the exact theory.

Many other theories have been developed and, in general, their complexity is directly proportional to their accuracy. These analyses are important because of the insight they give into the response of a cylinder subjected to impulsive loading. Knowing how stresses and displacements are distributed is crucial to the study of wave propagation and SHPB systems.

D. TRANSIENT BEHAVIOR

So far, the discussion has been limited to continuous waves or at least with pulses more than just a few cycles in length. However, in an SHPB experiment a very short pulse is propagated through the cylinder, giving rise to a transient behavior which cannot be completely determined from the continuous theories; therefore, a different approach must be taken. One way to tackle the transient problem is to use Fourier analysis. By decomposing the pulse into its continuous components, continuous wave theory can be used on each component at any point down the bar and the new pulse can be obtained by adding the pieces together again. This method is not exact but it does give a close approximation, especially at some distance from the source.

Choosing a mathematical function which describes the input pulse and which can be represented by a reasonably simple Fourier series is very difficult. Davies [27] used a trapezoidal pulse while Kolsky [28] assumed an error function. In both cases the Pochhammer and Chree curves are used to obtain the phase velocity for each pulse. To calculate the new shape of the wave-forms, only the fundamental mode is assumed to be excited.

Another approach taken by some investigators in studying transient behavior is based on the concept of "dominant groups" and the method of stationary phase. The idea is that if at the beginning everything is in phase, any time after that all waves are out of phase and, therefore, interfere destructively. When the combined effects of all these waves are studied, the main contribution comes from a small "dominant" group whose phase velocities, periods and wavelengths are almost the same. By focusing on this special group, one can obtain approximate propagation of longitudinal, flexural and torsional waves in a cylinder.

In this study the Fourier analysis approach was employed. It is straightforward and can be easily simulated numerically.

E. NUMERICAL ANALYSIS

Due to the complexity of even the solutions to a two-dimensional wave propagation problem, numerical methods must be employed to fully describe the response of an SHPB system.

Over the past 20 years many investigators have tried numerically to solve the governing equations of an SHPB system. The various finite-difference schemes are straightforward but tedious to derive. It seems pointless to start a numerical analysis from scratch. After having understood the physics and problems associated with a finite-difference approach, it does appear worthwhile to look and make use of available computer codes that were written specifically for this task. Considerable time and effort were spent in identifying and trying to obtain some of these programs. Two types of codes are available for this type of problems. The first specifically addresses the propagation of waves in a bar. The two most used are Toody [32] and Hemp which were written for a SHPB and could easily be adapted to the present needs. Unfortunately, they are quite old, hard to find, and not be as sophisticated and efficient as they

could be. The second group is of a more general kind; from these we could extract the modules of interest to this study, examples include Epic [31] and Hull [30].

Within the numerical arena contains is another worthwhile aspect of this study. Specifically, one can compute, solve, and present the Pochhammer and Chree solutions directly along the length of the bar. If their solution is correct, these results ought to match those of the governing equations numerical solutions.

Both numerical representations can tell us what the wave propagation looks like within the bar, and an analysis and feasibility assessment of a larger SHPB will be possible. What is of interest is the distribution of radial stresses and strains at different stations along the bar to decide whether a one-dimensional analysis is still reasonable or not. Furthermore, the effects of friction and specimen inertia and their relationship to the specimen size can be studied.

Because of the enormous complexity of the analytical solutions, the computational approach is not only a valuable but an indispensable tool. A comparison and analysis of the exact solutions, and of the finite difference solution of the governing equations will give a complete look at and understanding of an SHPB system, and recommendations will be possible regarding a "larger" bar.

F. COMPROMISES

Looking beyond the general equations of wave propagation in a long cylindrical bar, focus is placed on the SHPB system. Understanding the mathematical background makes it apparent that the analyst must make many compromises. One problem may be minimized and another may be magnified to reach some basic assumption, and an important part of the system may be ignored.

For example, to minimize inertia the material specimen to be tested should be as short as possible. To minimize friction, the length-to-diameter ratio of the specimen should be high. When the material is concrete, a length-to-diameter ratio close to one should be used in order to have the same number of aggregates in both directions. This poses a problem for the experimenter who must choose in essence which errors will be introduced in the system. By minimizing friction, inertia will play an important role; the reverse is also true. To properly test concrete, neither friction nor inertia can be minimized. In the system as a whole, it has been shown that to minimize dispersion the diameter should be much less than the wave length, that is the duration of the input pulse should be long compared to the time taken for the pulse to travel a distance equal to the radius. Also, the duration of the pulse should be much greater than the transit time through the specimen. This last restriction arises from momentum considerations, and goes back to the basic SHPB assumption of conversation of momentum across the specimen.

The Pochhammer and Chree equations show that the longitudinal stresses and displacements will vary radially and their distribution along the cross section is directly dependent on the frequency of the pulse. Since measurements in an SHPB are made on the surface and assumed constant throughout the radial distance, large errors could be introduced depending on the specific conditions.

Radial inertia has also been addressed by several investigators, it is probably due to the kinetic energy but its effects are unknown.

Finally, it has always been assumed that only the fundamental mode of vibration is excited in a typical SHPB. This appears true for the conditions in the experimental setup, and analyses based on mode 1 only have shown good correlation to experimental data.

SECTION III

A. DISCUSSION

The particle motion in a bar is governed by the equations of motion. Pochhammer and Chree independently solved these equations for the propagation of a sinusoidal wave. The solution, discussed in section II.A is the so called frequency equation; it has an infinite number of solutions, one for each mode, and results in a function relating Cp, Λp and ν [wave speed, wave length and Poisson's ratio]. These solutions are valid and exact for infinitely long bars. If the bar is long enough to eliminate end effects (10 diameter lengths) and if the interest is in the transient pulse in its first passage, then the infinite assumption is pretty good.

The Pochhammer and Chree solutions can be plotted in non-dimensional form as shown in Figure 1. It is interesting to note that since $\Lambda = c_p T$, *then* $\frac{a}{\Lambda} = \frac{a}{c_p T}$ and *thus* $\frac{a}{\Lambda}\frac{c_p}{c_o} = \frac{a}{T c_o}$;

then if a is multiplied by a certain factor and T is also multiplied by that same factor, then $\frac{a}{\Lambda}$ *vs* $\frac{c_p}{c_o}$ will not change. What this means is that mathematically, under the assumptions made, if the diameter is increased to 6 inches and simultaneously the duration of the input pulse is increased by the same factor, then the solution is the same. This applies to a sinusodial, continuous input where the wavelength is constant, and thus, it will travel at only one wavespeed relative to the bar radius: a long wave in a large bar will have the same wave speed as a short wave in a small bar. As long as $\frac{a}{\Lambda}$ stays constant, nothing changes.

What happens if the input is a transient pulse? A simple mathematical function can be chosen to describe this type of input and it can be represented by a Fourier series. A transient pulse is composed of a spectrum of frequencies; the higher

frequency components travel more slowly than the lower frequency components, and thus lag behind and cause the initial sharp pulse to spread. This spreading is called dispersion. The Pochhammer and Chree solutions give the velocity of each wave depending on its frequency, and thus one can correct for dispersion by calculating how far each frequency component has traveled in a certain time, and then reassemble the pulse. This task basically amounts to correcting for phase changes within each term of the Fourier series. It is important to be able to correct for dispersion since the strain gages recording the pulse are typically 30 to 60 inches from the specimen. Interest is in the response at the specimen itself but in many cases a gage cannot be physically placed there. The dispersion correction technique allows one to predict the shape of the pulse as it travels from the strain gage to the specimen.

Further, following the same kind of reasoning as for the continuous wave case, $\frac{a}{\Lambda}\frac{c_p}{c_0} = \frac{a\pi}{n\,\Delta t\,c_0}$ can be written where n is the number of points taken to represent the transient pulse and Δt is the time interval between them. In essence $n\,\Delta t$ is the period of the transient pulse, and if $\frac{a}{n\,\Delta t}$ stays constant, the case is analogous to the continuous case, as long as the radius and the pulse width are increased or decreased by the same amount, the problem will not change.

This fact is important to this study because the main concern is the feasibility of a 6-inch SHPB system. What the Pochhammer and Chree equations show is that if the incident pulse is of large enough duration then, at least as far as the longitudinal waves are concerned, there is mathematically no difference between a 2-, 3-, 6- or 60-inch diameter SHPB. One must then determine what pulse duration would be needed to make a new 6-inch system equivalent to the existing 2- and 3-inch bars and whether a pulse that long can be produced. The answer to the question of pulse period needed is fairly straightforward.

Analyses of the bars and input pulses used both at Tyndall AFB and at the University of Florida, showed that a 6-inch system would be equivalent to the existing ones, if the input pulse duration was roughly 500 μsec .

From conservation of momentum consideration, the length of the striker bar is related to the pulse duration as $T = 2L_s/c_0$ where C_o is the elastic wave speed and L_s is the striker bar length.

This means that for a steel SHPB incident a pulse of 500 μsec , a 50-inch long striker bar would be required. It is not the author's responsibility to assess the feasibility of a bar this size, however it appears that there will be problems associated with it especially in obtaining a perfectly centered impact.

Another concern in a typical SHPB, is how much the stresses and displacements vary along the cross section. As mentioned earlier, a uniform distribution is assumed, and only strains on the surface are measured. It is then very important to identify under which conditions the one-dimensional assumption is acceptable. Davies [27] computed the ratio of the longitudinal displacement at the surface to that along the axis and showed that for $\frac{a}{\Lambda}$ less than 0.1 their difference is less than 5 percent. For a continuous pulse, with one value of Λ , one-dimensionality is assured if $\frac{a}{\Lambda} \le 0.1$. When dealing with a transient wave where many pulses exist, "most of them" or the terms in the Fourier expansion with greatest contribution must be in the $\frac{a}{\Lambda} \le 0.1$ region to insure one-dimensionality. One way to check this is to print out $\frac{a}{\Lambda}$ values for each Fourier component and look at the corresponding amplitude ratios. The goal is to have them quite small by the time $\frac{a}{\Lambda}$ reaches 0.1. But what does "quite small" mean? Ten percent of the original amplitude? One percent? To answer this question, a short computer code was written to calculate $\frac{a}{\Lambda}$ values and Fourier amplitude for an assumed trapezoidal input based on the Pochhammer-Chree

solutions. This allowed one to look at the values for the existing systems at the University of Florida and at Tyndall AFB; it was found that the amplitudes of the Fourier components had fallen to 5-9 percent of the original value by the time $\frac{a}{\Lambda}$ reached 0.1. Therefore, a good value to use for the proposed 6-inch system is about 10 percent. This would assure the one-dimensionality of the response. Notice that it does not matter at which component $\frac{a}{\Lambda}$ reaches 0.1, but rather the value of the amplitude at that point. If it is at the 10th or the 100th term in the Fourier series it makes no difference.

As a check, calculations were made for a 6-inch bar and 500 μsec input pulse, and, as predicted from our earlier discussion, the amplitude of the Fourier components drop off to 8 percent of their original value before $\frac{a}{\Lambda}$ becomes 0.1. This is shown in Table A-1 in the Appendix for three bars, nominally a 2-inch, a 3-inch and a 6-inch bar, for an assumed trapezoidal input of normalized amplitude of 1. Also included in the appendix is the comparison of corrected waveforms for a 2-inch bar with a 250 μsec pulse and a 6-inch bar with a 750 μsec pulse, to show the similarity, while a 6-inch bar with a 200 μsec pulse clearly shows the deviation from one-dimensionality.

B. CORRECTIONS

Up to this point the aspects of wave propagation in a cylindrical bar have been discussed. It has been established that by choosing a pulse of a certain duration, the conditions of a typical SHPB can be reproduced in a 6-inch diameter system. It was shown that dispersion corrections can still be made assuming only mode 1 vibrations and that the one-dimensional assumption is still valid. The only provision is for the bar to be long enough to avoid end effects.

A SHPB has, by definition, a specimen in between and in contact with the input and the output bars. The specimen will contribute inertia to the problem as well as errors due to friction. As discussed in section II, there are ways to minimize the effects of friction and/or inertia. To minimize friction a good rule of thumb is to maintain $\frac{\mu d}{3L} << 1$. The values of μ are not quite known, and certainly not constant for any one case, but from this the radius and the length of the specimen should be a minimum, be of the same order of magnitude. Keeping that in mind, we turn our attention to inertia; radial inertia is assumed to cause a larger stress than that which would have resulted in its absence. Davies and Hunter [7] calculated the contribution of inertia based on the kinetic energy due to both axial and radial motions. Their result is

$$\sigma_s = \sigma_b + \rho_s \left(\frac{L^2}{6} - \nu_s^2 \frac{d^2}{8} \right) \frac{d^2 \varepsilon}{dt^2} \qquad (18)$$

where σ_b is the measured stress, subscript s pertains to the specimen and $\frac{L^2}{6}$ and $\nu_s^2 \frac{d^2}{8}$ are the axial and radial inertia contributions respectively.

The length and the diameter of the specimen can be chosen so that the second part of Equation 18 vanishes; thus the effects of inertia and minimized. That is

$$\frac{L^2}{6} = \nu_s^2 \frac{d^2}{8}$$

which leads to $\frac{L}{d} = \frac{\sqrt{3}}{2} \nu_s$ (19)

For concrete, as an example, ν_s is roughly .22 and thus one would want an $\frac{L}{d} \cong .2$.

This result is consistent with the friction considerations, but unfortunately not with the testing procedures for concrete. A very important factor in this material is aggregate size and number. To properly test concrete the number of aggregates must be the same in both directions; thus an L/d of one is usually recommended. Therefore, both for a 2-inch as well as for a 6-inch SHPB, inertia effects cannot be cancelled. Therefore, inertia effects cannot be cancelled for either a 2- or 6-inch SHPB.

For a large system, like the one proposed, the inertia effects cannot be ignored and the analyst would have to calculate the contributions, based on the measured $\frac{d^2\varepsilon}{dt^2}$, and add it to the measured stress. Because quantities are known, this should not be difficult.

Additionally, several investigators have calculated the effects of radial friction and an additional contribution due to inertia from the convective portion of the material derivative. Both were found to be insignificant in a typical SHPB. This is believed to hold true for a 6-inch system because the diameter appears in the equation as $\frac{d}{L}$ ratio, which is kept to about one in all cases.

C. NUMERICAL RESULTS

The Lagrangian module in the hydrocode Hull [ ] was exercised to numerically solve the equations of motion in a 6-inch elastic bar subjected to a step input pressure. The enormous amount of calculations in the code requires many hours of CPU time for just a few microseconds of calculations.

The goal of this exercise was to answer two questions. Is the motion one-dimensional and is it uniform in the radial direction? These questions are important because they can validate the conclusions made in the mathematical analysis and thus reinforce the allegations of feasibility of a 6-inch system.

Figures 3 and 4 show the longitudinal stresses and strains at the surface and in the center of the bar. Figures 5 and 6 show all the stresses at those same points. All output was calculated roughly 50 inches (1.27 m) from the impacted end, and the problem was run for a millisecond. Figures 3 and 4 confirm the fact that the stresses do not vary appreciably along the cross section, while Figures 5 and 6 confirm the one-dimensionality of the response, as all but T_{yy}, the longitudinal stress, are quite insignificant.

These results are a direct outcome of the finite differencing of the actual governing equations, and, as such, provide a reliable tool to compare results obtained via approximate solutions and other simplifying assumptions.

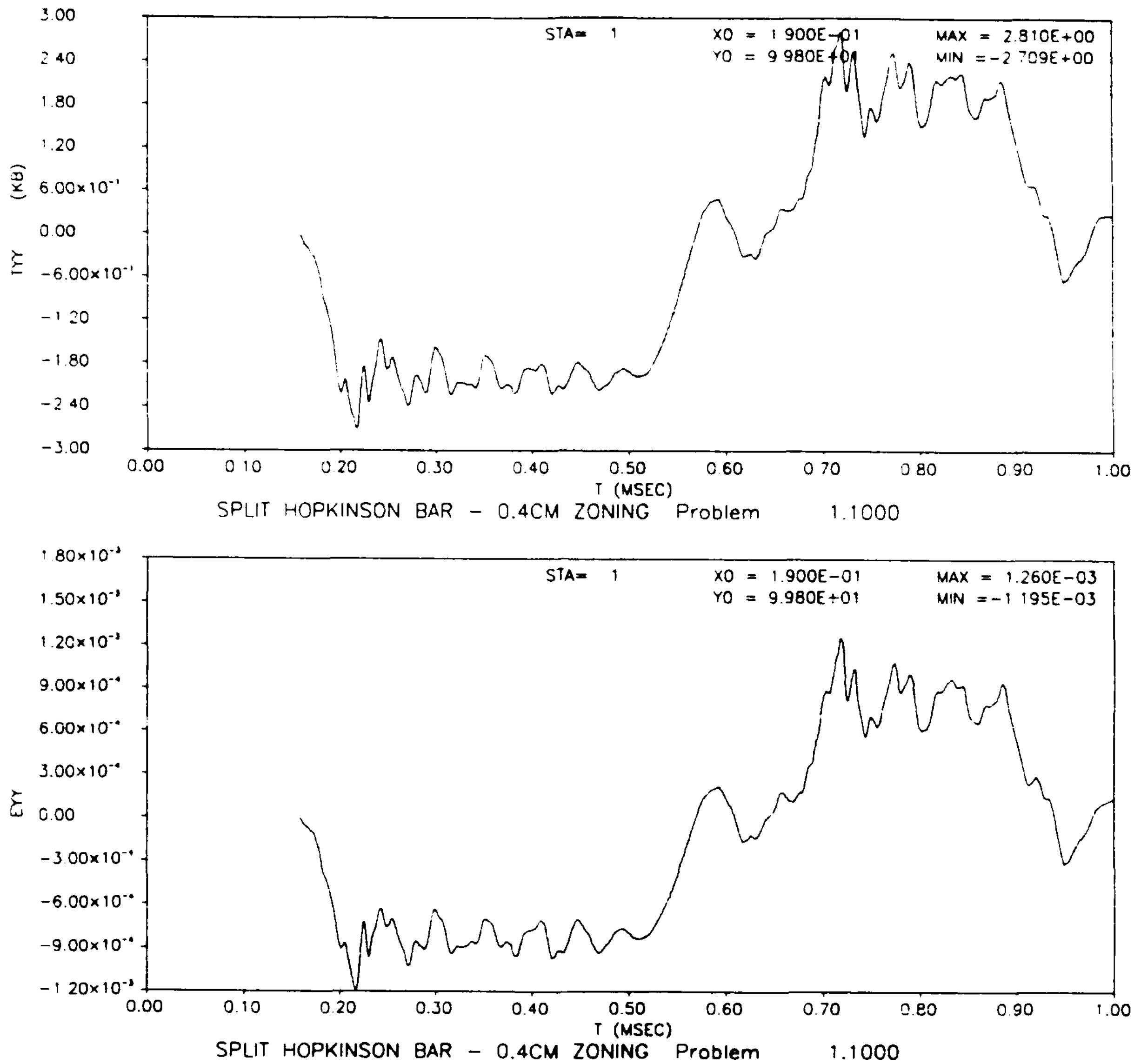

Figure 3. Longitudinal Stress and Strain at the Center.

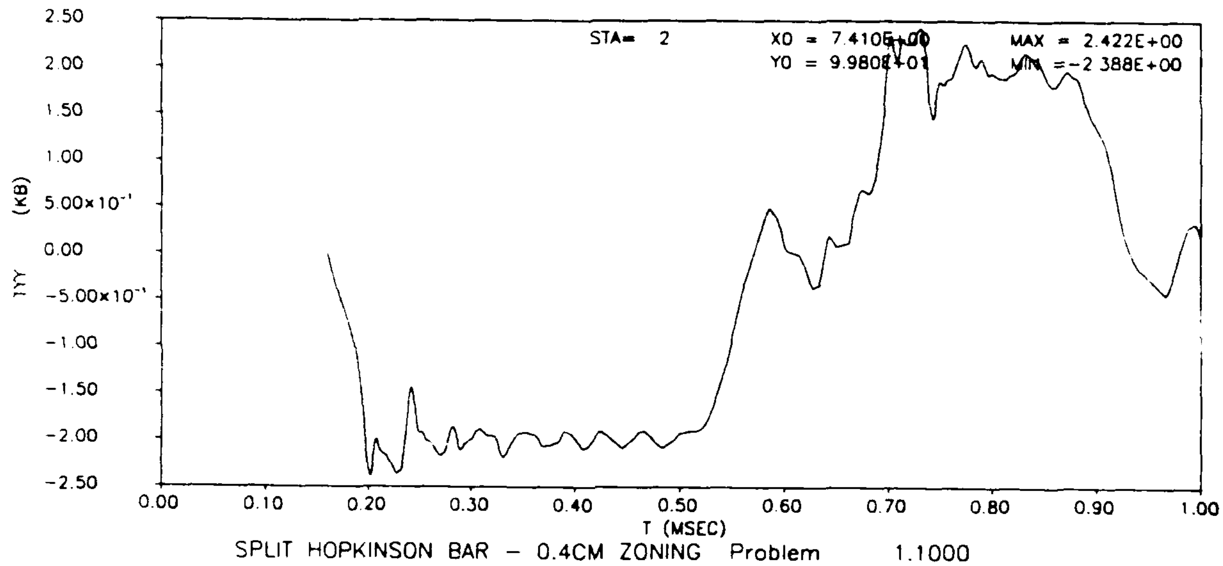

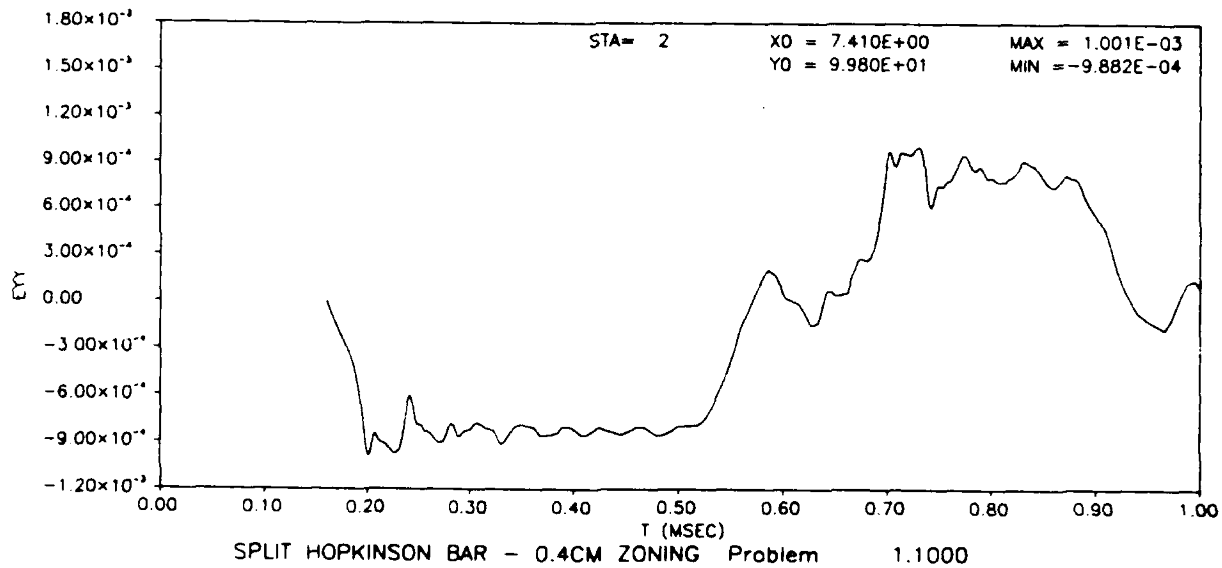

Figure 4. Longitudinal Stress and Strain at the Surface.

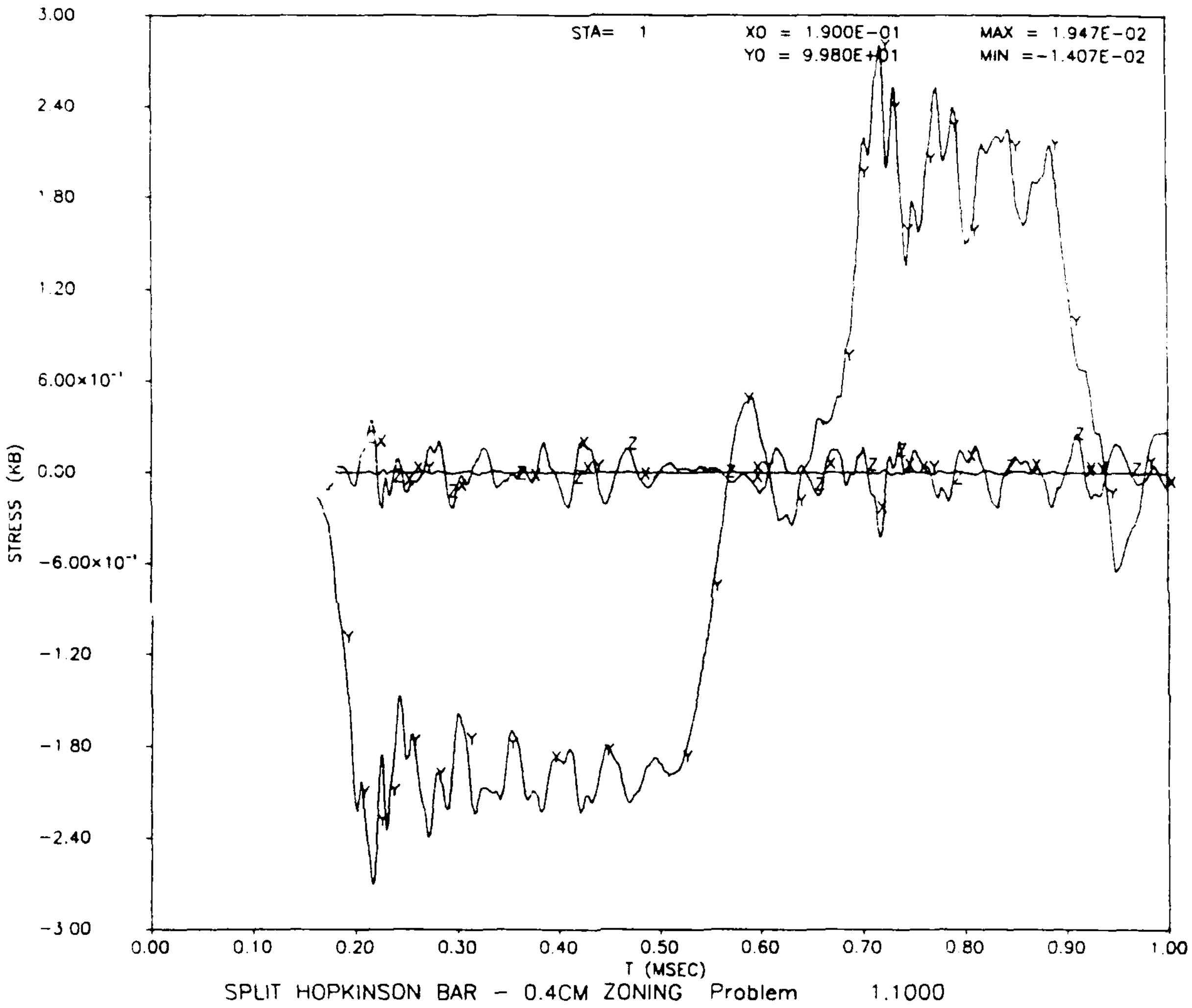

Figure 5. Stresses at the Center of Bar.

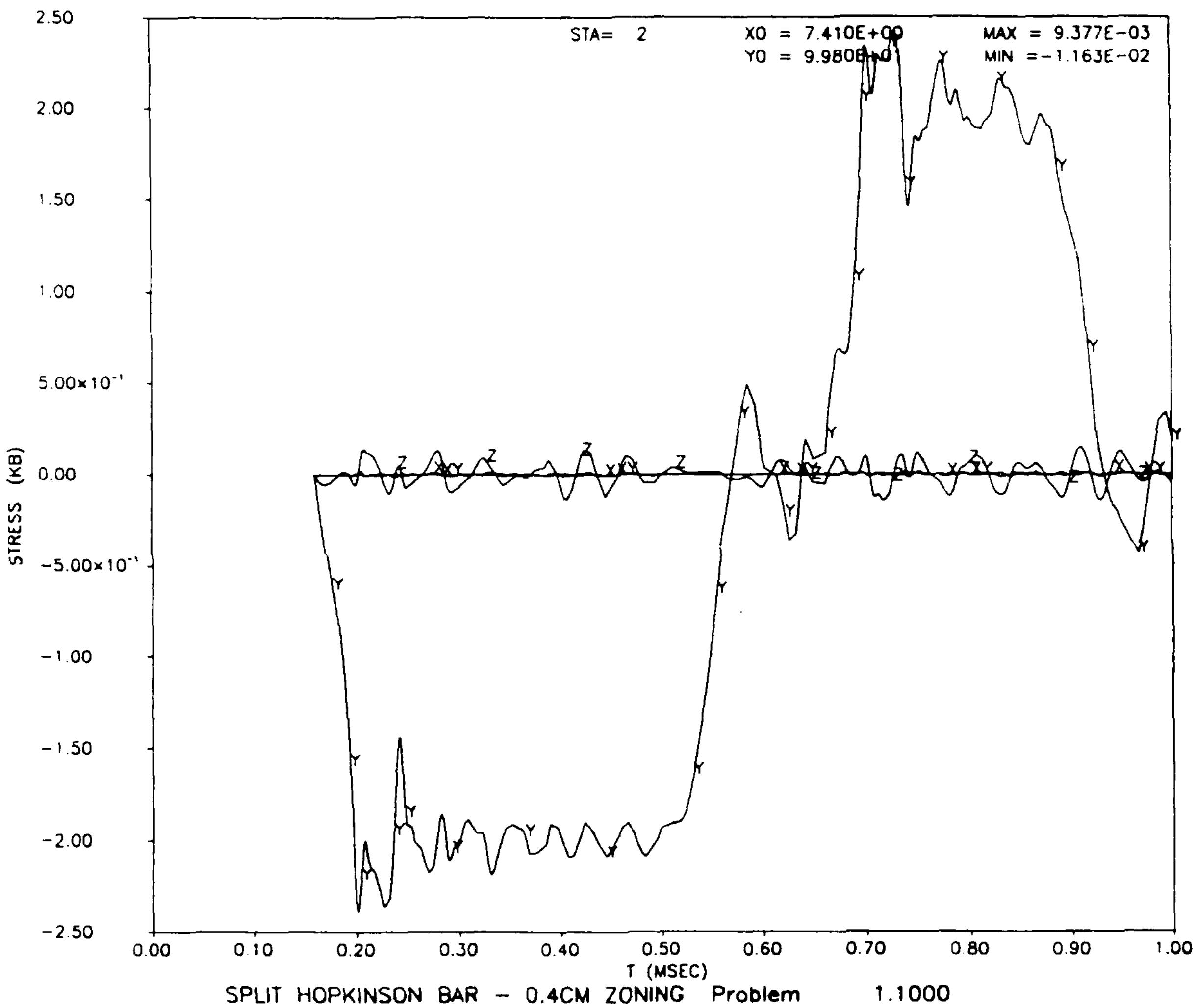

Figure 6. Stresses at the Surface.

SECTION IV

CONCLUSIONS/RECOMMENDATIONS

The major question to be answered in this effort was whether a 6-inch SHPB is feasible, do the assumptions for a 3-inch system still apply and what are the problems and issues associated with a system of that size.

The author believes that, because of the form of the equations involved, a pressure bar system can be scaled up or down to any degree, without affecting particle motion. It was shown that a pulse 500 μsec in duration in a 6-inch bar is mathematically identical to a 250 μsec pulse in a 3-inch bar.

This does not mean the response is perfectly one-dimensional, nor does it exactly follow the Pochhammer-Chree solutions. What it does imply, however, is that since the existing 2- and 3-inch SHPB have been shown to give reliable results, and thus validating the basic assumptions made, then the proposed 6-inch system will be just as accurate and useful.

Where a larger system will differ from a smaller one is in the treatment of the specimen. In compression the specimen is not attached to the main bars, and thus friction and inertia contribute some errors to the analysis. It seems logical that the heavier the specimen the greater kinetic energy it will have; so, in a 2-inch system where friction and inertia are probably negligible, in a 6-inch system they are not. This study proposes a way to correct for inertia as discussed in section IIIA. It further appears from experimental results, that the strain rate eventually levels off to a quasi - steady state value, so that its derivative with respect to time which appears in Equation (18), may eventually go to zero, thus minimizing inertia effects automatically.

One could also argue about the difficulty in having a striker bar over 4 feet long and 6 inches in diameter. Although not in the scope of this study, two suggestions come to mind. A sleeve or barrel could be manufactured to guide the striker bar and assure a centered impact. Secondly there are other means of inputting a pressure pulse in a bar other than from a bar's impact. A little creativity may bypass a lot of complications associated with scaling up existing methods.

Finally, more numerical calculations could prove useful in studying the effects of radial constraints and friction, and give a better understanding of stress/strain distributions in a large diameter SHPB.

REFERENCES

1. Kolsky, H., "An Investigation of the Mechanical Properties of Materials at Very High Rates of Loading," Proceedings of the Physics Society, Vol. 62, 1949.

2. Hauser, F.E., Simmons, J.A., and Dorn, J.E., "Response of Metals to High Velocity Deformation," Proceedings of the Metallurgical Society Conference, Vol. 9, 1960.

3. Lindholm, U.S., "Some Experiments with the Split Hopkinson Pressure Bar," Journal of the Mechanics and Physics of Solids, Vol. 12, 1964.

4. Malvern, L.E., and Ross C.A., "Dynamic Response of Concrete and Concrete Structures," Final Technical Report, AFOSR Contract F49620-83-K007, May 1986.

5. Robertson, K.D., Chou, S. and Rainey, J.H., "Design and Operating Characteristics of a Split Hopkinson Pressure Bar Apparatus," Technical Report AMMRC TR 71-49, November 1971.

6. Kolsky, H., Stress Wave in Solids, Dover Publications, New York, 1963.

7. Davies, E.D.H., and Hunter, S.C., "The Dynamic Compression Testing of Solids by the Method of the Split Hopkinson Pressure Bar," Journal of the Mechanics and Physics of Solids, Vol. 11, 1963.

8. Rand, J.L., U.S. Naval Ordnance Laboratory Report, NOLTR67-156, 1967.

9. Dharan, C.K.H. and Hauser, F.E., Experimental Mechanics, Vol. 10, pp. 370, 1970.

10. Samanta, S.K., Journal of the Mechanics and Physics of Solids, Vol. 19, pp. 117, 1971.

11. Jahsman, W.E., "Re-examination of the Kolsky Technique for Measuring Dynamic Material Behavior," Journal of Applied Mechanics, Vol. 38, 1971.

12. Chiu, S.S. and Neubert, V.H., Journal of the Mechanics and Physics of Solids, Vol. 15, pp. 177, 1967.

13. Young, C. and Powell, C.N., "Lateral Inertia Effects on Rock Failure in Split Hopkinson-Bar Experiments," 20th U.S. Symposium on Rock Mechanics, 1979.

14. Nicholas, T., "An Analysis of the Split Hopkinson Bar Technique for Strain-Rate-Dependent Material Behavior", Journal of Applied Mechanics, March 1973.

15. Lawson, J.E., "An Investigation of the Mechanical Behavior of Metals at High Strain Rates in Torsion," Ph.D. Dissertation, Air Force Institute of Technology, June 1971.

16. Baker, W.E. and Yew, C.H., "Strain-Rate Effects in the Propagation of Torsional Plastic Waves", Journal of Applied Mechanics, Vol. 33, 1966.

17. Jones, R.P.N., "The Generation of Torsional Stress Waves in a Circular Cylinder", Quarterly Journal of Mechanics and Applied Mathematics, Vol. 12, 1959.

18. Okawa, K., "Mechanical Behavior of Metals Under Tention-Compression Loading at High Strain Rate", Aeronautical Engineering, Kyoto University, Kyoto, Japan 606, 1984.

19. Ross, C.A., Nash, P.T., Friesenhahn, G.H., "Pressure Waves in Soils Using a Split-Hopkinson Pressure Bar", Final Technical Report, ESL-TR-81-29, July 1986.

20. Rajendran, A.M. and Bless, S.J., "High Strain Rate Material Behavior", Technical Report, AFWAL-TR-85-4009, December 1985.

21. Ross, C.A., "Split Hopkinson Pressure Bar Tests," Final Technical Report, ESL-TR-88-82, March 1989.

22. Follansbeen, P.S. and Frantz, C., "Wave Propagation in the Split Hopkinson Pressure Bar", ASME Journal of Engineering Materials and Technology, Vol. 105, 1983.

23. Bertholf, L.D. and Karnes, C.H., "Two-dimensional Analysis of the Split Hopkinson Pressure Bar System," Journal of the Mechanics and Physics of Solids, Vol. 23, 1975.

24. Karal, F.C., "Propagation of Elastic Waves in a Semi-infinite Cylindrical Rod Using Finite Difference Methods," Journal of Sound Vibration, Vol. 13, 1970.

25. Bancroft D., The Velocity of Longitudinal Waves in Cylindrical Bars, Physical Review, Vol. 59, April 1941.

26. Mindlin, R.D. and Herrmann G., A One-Dimensional Theory of Compressional Waves in an Elastic Rod, Pro. 1st U.S. Nat. Gong. App. Mech., Chicago, 187-191, 1951.

27. Davies, R.M., 1948, A Critical Study of the Hopkinson Pressure Bar, Philosophical Transactions Royal Society A240, 375-457.

28. Kolsky, H., 1956, The Propagation of Stress Pulses in Viscoelastic Solids, Phil. Mag. 1, 693-710.

29. Love, A. E. H., 1927, The Mathematical Theory of Elasticity, Dover Publications, New York.

30. Hull, Finite Difference Code, Orlando Technology, Inc., Box 855, Shalimar, Florida 32579.

31. Epic, Elastic Plastic Impact Calculation, G. R. Johnson, R. A. Stryk, Honeywell, Inc., Armament Systems Division, 7225 North Land Drive, Brooklyn Park, Minnesota 55428.

32. Toody IV, A Computer Program for Two Dimensional Wave Propagation, J. W. Swegle, Computational Physics and Mechanics Division I-5162, Sandia Laboratories, Albuquerque, New Mexico 87185.

APPENDIX A

TABLE A-1. AMPLITUDES AND RADIUS OVER WAVELENGTH VALUES FOR 2, 3, AND 6 INCH BARS

	Duration -->	250 μsec	250 μsec	1000 usec
	Bar Diameter -->	2-inch	3-inch	6-inch
n	An/Ao	$\frac{a}{\Lambda}$		
1	-.635	.0105	.0154	.0076
2	.2116	.0316	.0464	.0228
3	-.1263	.0528	.0776	.038
4	.0895	.0741	.1092	.0533
5	-.0689	.0956	.1418	.0686
6	.0556	.1174		.0841
7	-.0463	.1397		.0997
8	.0394			.1154
9	-.0340			.1314
10	.0297			

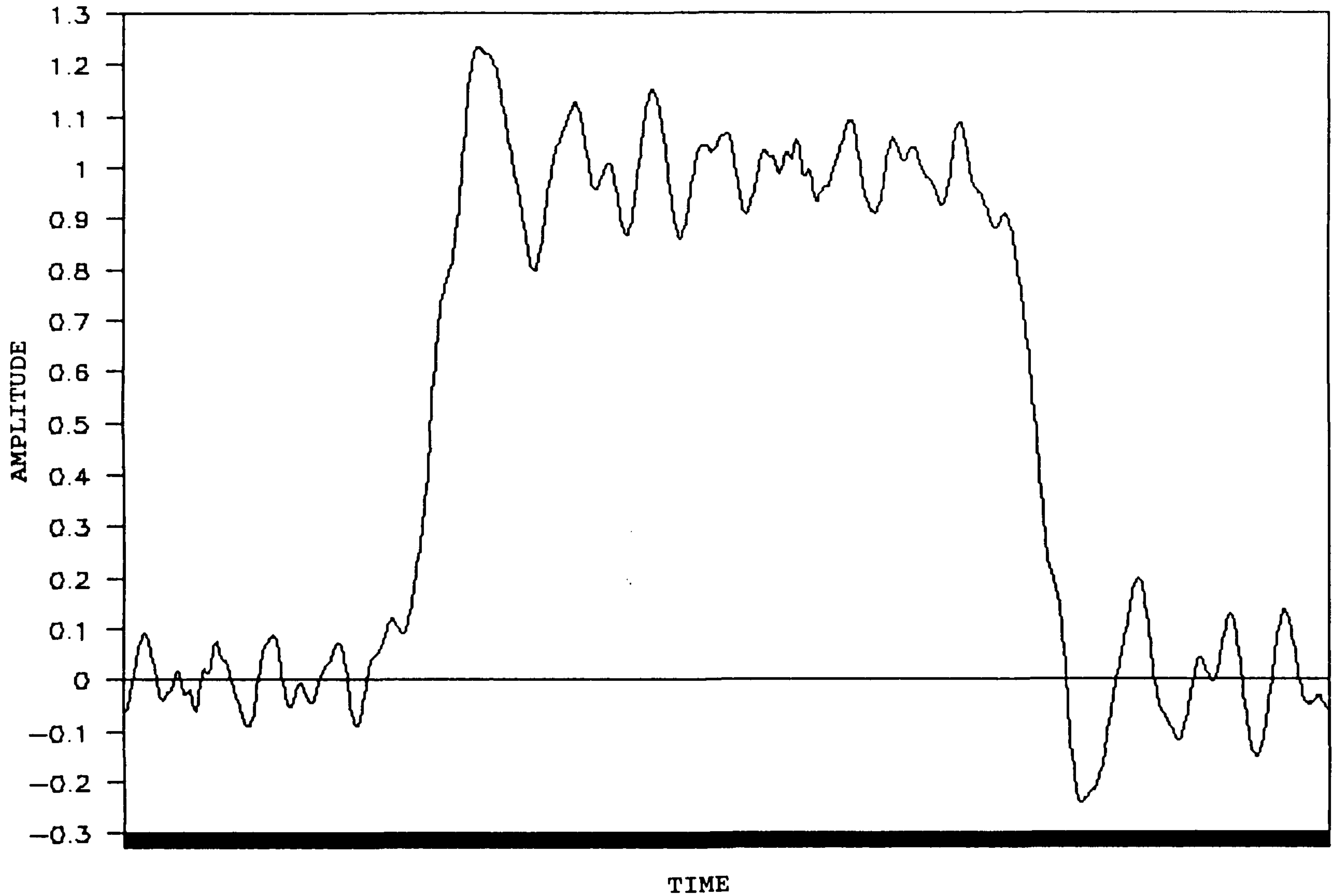

Figure A-1. TYNDALL BAR (2 inches, 250 μsec).

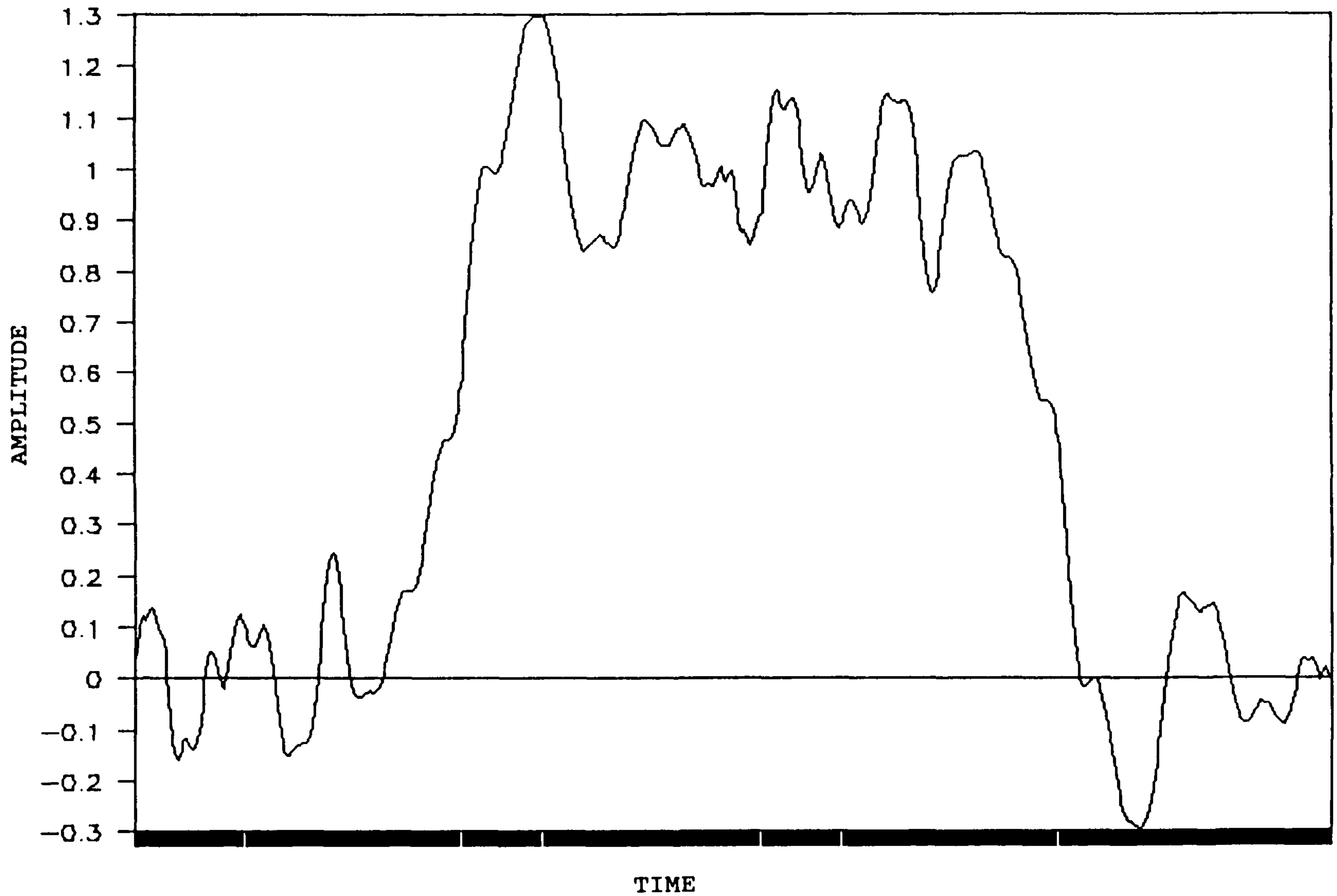

Figure A-2. TYNDALL BAR (2 inches, 160 *μsec*).

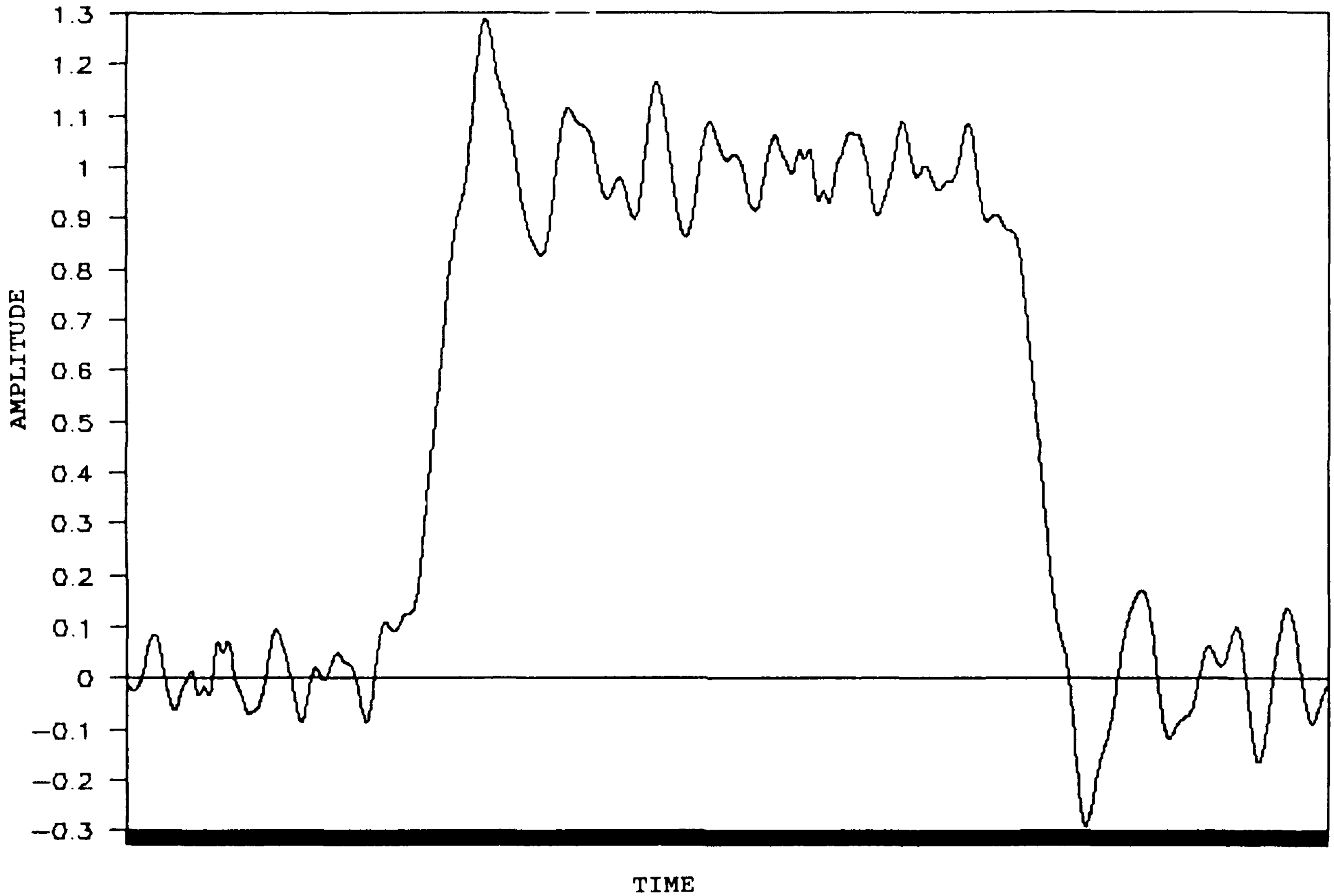

Figure A-3. 6-INCH BAR (750 μsec).

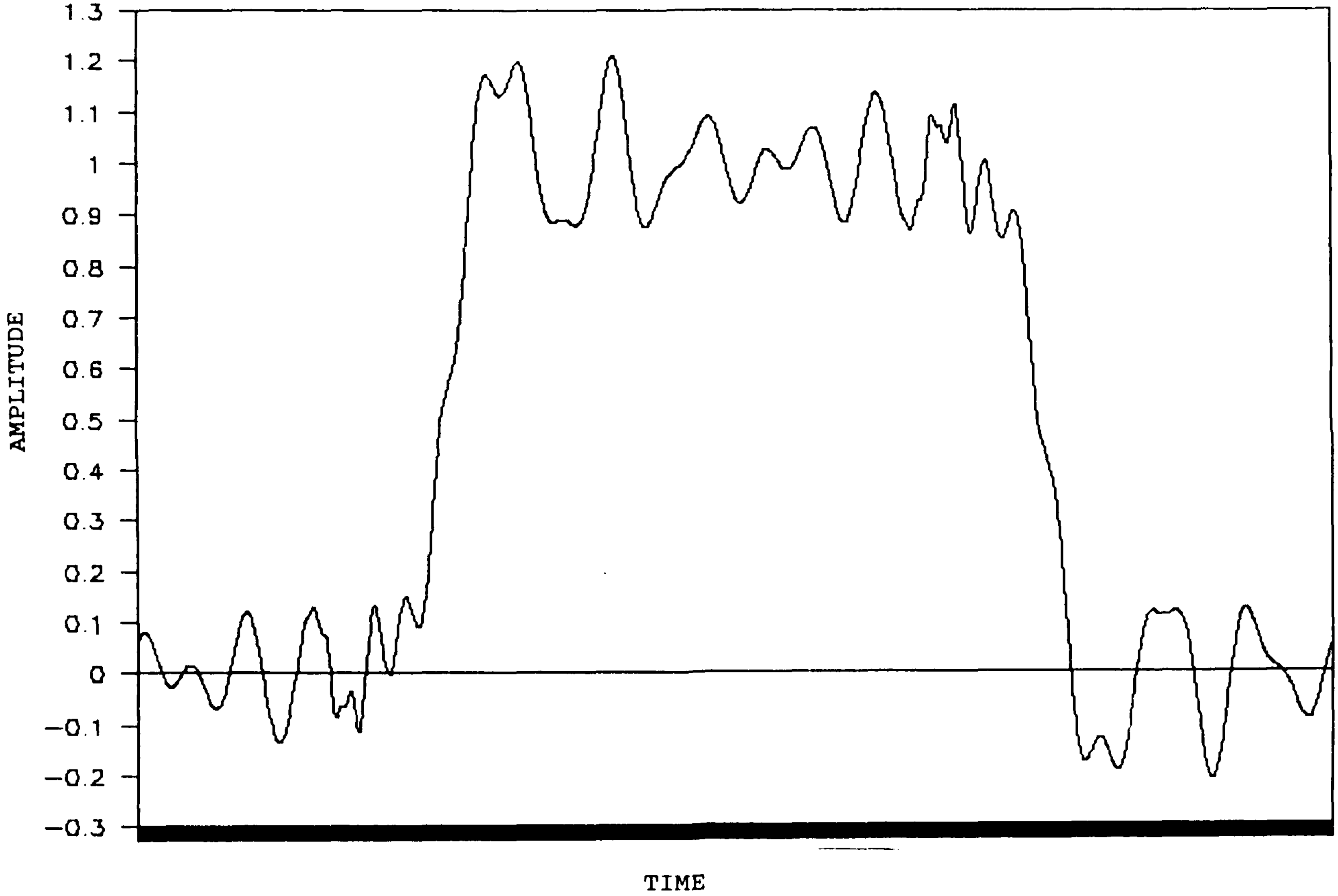

Figure A-4. 6-INCH BAR (500 μsec).

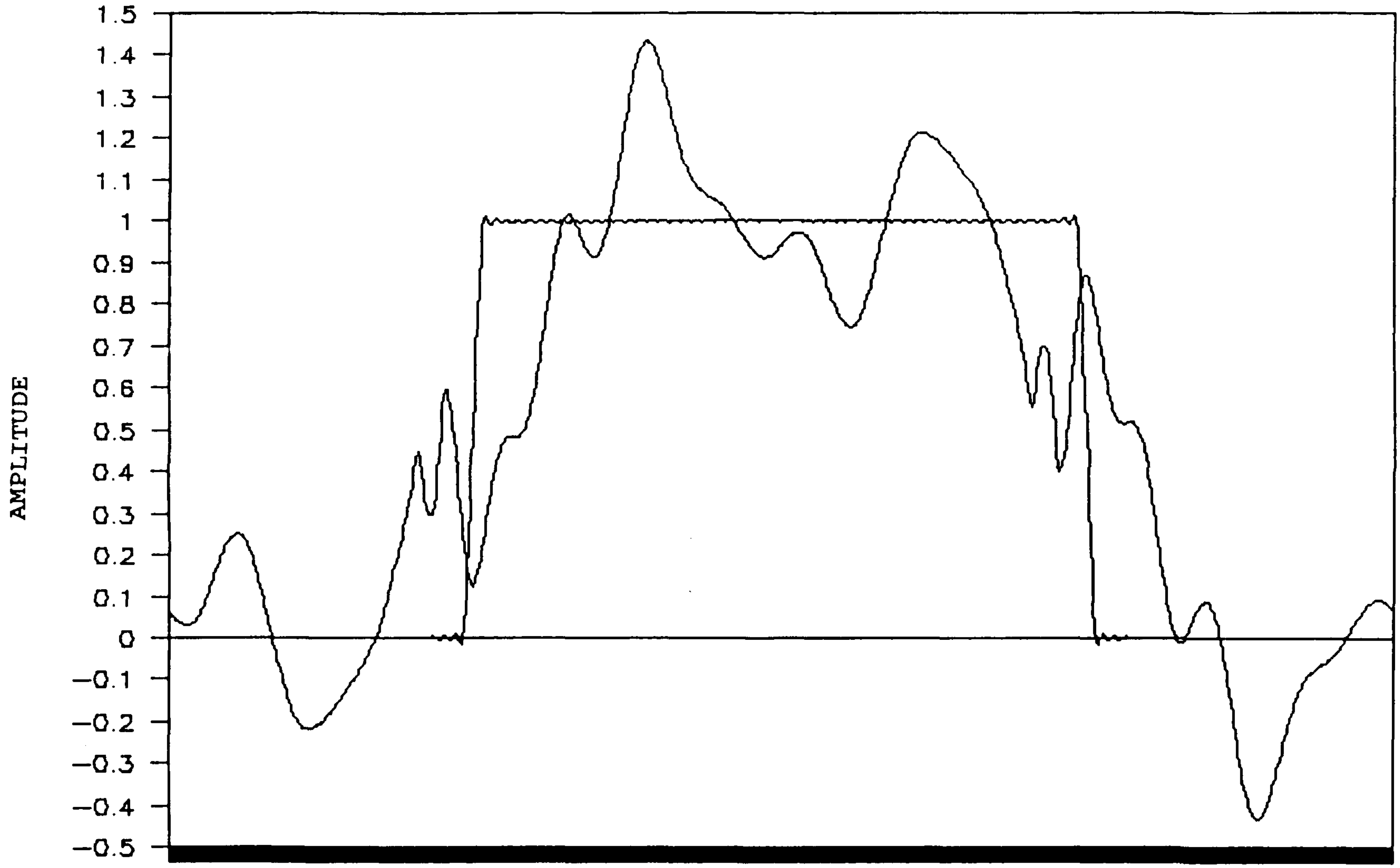

Figure A-5. 6-INCH BAR (200 μsec).